❒   20

Research on neutral-point potential control of a three-level inverter

Guangjie Fu, Xinpeng Li
School of Electrical and Information Engineering, Northeast Petroleum University, Heilongjiang Province, China

Article Info	ABSTRACT
	Diode-clamped three-level inverters have been widely used in high voltage and high power fields because of their unique advantages. Nowadays, diode-clamped three-level inverters have become a research hotspot. The imbalance of midpoint potential and complex control strategies have become the choke point of its development. In order to reduce the content of energy harmonics injected into the power grid by the inverter system, the neutral point potential needs to be controlled. This paper proposes a control method based on a proportional controller. The voltage sector was redefined and the design of the proportional controller was completed. In combination with the introduction of a new PWM technology, a smooth control of the midpoint potential was achieved. The effectiveness of the method is verified by simulation in MATLAB.

Corresponding Author:

Guangjie Fu,
School of Electrical and Information Engineering,
Northeast Petroleum University,
Daqing, Heilongjiang Province, China.
Email: fgjmhw@163.com

1. INTRODUCTION

With the ever-decreasing reserves of fossil energy, new energy sources are increasingly favored by people. The installed capacity of photovoltaic power generation is increasing, and photovoltaic grid-connected inverter technology has become a research hotspot [1]. Compared with two-level inverters, three-level inverters have large output capacity, strong anti-interference, and small switching loss, which can improve the quality of the output waveform and reduce the harmonic content of the output [2]-[4] Due to these characteristics of the Neutral Point Clamped (NPC) type three-level inverter, it has been widely used in photovoltaic inverter grid-connected [5]-[6], and the midpoint potential control is one of its important research topics.

The commonly used midpoint potential control methods are hardware method and software method [7]-[10]. The hardware algorithm is to add a plurality of DC power supplies or increase DC capacitance on the DC side. The software algorithm controls the midpoint potential through the design of the control algorithm. Compared with the software method, the hardware method has high hardware cost and the software method is easy to implement [11]-[14]. Commonly used software controls include multi-carrier PWM method, specific harmonic elimination PWM method, and space vector PWM method. These methods have complicated operation or unstable DC-side current, which limits the quality of inverter output power [15]-[18]. This paper uses a proportional controller and a new PWM technology to control the midpoint potential. Finally, the effectiveness of the method is verified by simulation.

2. SYSTEM MODEL

The inverter system is mainly composed of photovoltaic cells, NPC type three-level inverters and AC power grid. The structure of the inverter control system is shown in Figure 1.
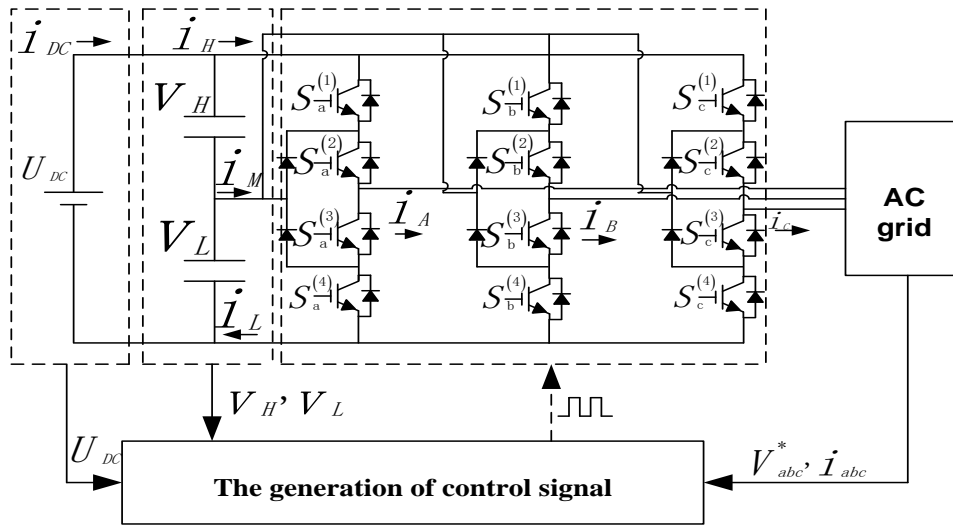
Figure 1. Inverter system control flow chart

2.1. DC-link voltage control model

As can be seen from Figure 1, each bridge of the NPC type three-level inverter includes four switches and two clamping diodes. The high-voltage side and the low-voltage side share the DC-link voltage. The voltages are respectively represented by V_H and V_L, and the voltage at the end of the phase is represented by V_x, H and L respectively represent the states of different bridge arms. The definition of each state is shown in the following Table 1.

Table 1. Definition of leg status

Leg status	switch status				Terminal voltage
	$S_x^{(1)}$	$S_x^{(2)}$	$S_x^{(3)}$	$S_x^{(4)}$	
H(V_H)	ON	ON	OFF	OFF	Udc/2
L (V_L)	OFF	OFF	ON	ON	-Udc/2

Where, X∈{a,b,c}.
Therefore, the voltage of each phase can be defined as follows:

$$V_x = \delta_H V_H - \delta_L V_L, X \in \{\alpha, \beta, \gamma\} \tag{1}$$

Where δ_H、δ_L respectively represent the working periods of the bridge in the high and low states, $\{\alpha, \beta, \gamma\}$ represents the working period of bridge $\{a, b, c\}$, and the working period of each bridge must satisfy the condition: $\delta_H + \delta_M + \delta_L = 1$.

$$-V_L \leq V_x \leq V_H, x \in \{a, b, c\} \tag{2}$$

Where V_H and V_L can be expressed as follows:

$$\begin{cases} \dfrac{dV_H}{dt} = \dfrac{i_{DC} - i_H}{C} \\ \dfrac{dV_L}{dt} = \dfrac{i_{DC} - i_L}{C} \end{cases} \tag{3}$$

By subtracting the two ends of the formula above :

$$\frac{dV_M}{dt} = \frac{i_M}{C} \tag{4}$$

Where $V_M = V_H - V_L$, $i_M = i_H - i_L$.

The final DC-link current can be expressed as follows:

$$\begin{cases} i_H = \alpha_H i_a + \beta_H i_b + \gamma_H i_C \\ i_L = -\left(\alpha_L i_a + \beta_L i_b + \gamma_L i_C \right) \end{cases} \tag{5}$$

From equation (4), it can be seen that the imbalance of the neutral point potential can be controlled by i_M , so that it can be controlled by an appropriate PWM technique using a proportional controller. Therefore, the binary definition of the voltage sector is introduced in this paper, and a new parameter $\{u, v, w\}$ is introduced as shown in Table 2.

Table 2. Terminal index of each phase

σ_V	I	II	III	IV	V	VI
u	a	c	b	a	c	b
v	b	a	c	b	a	c
w	c	b	a	c	b	a

Where V_{uv} represents the maximum voltage value, and V_{vw} and V_{wu} are always opposite to V_{uv}. Therefore, from formula (1):

$$V_x = \delta_H V_H - \delta_L V_L, -V_L \leq V_x \leq V_H \tag{6}$$

Where $X \in \{u, v, w\}$, $\delta \in \{\varphi, \psi, \xi\}$, δ represents the working period of X. Assuming that the H and L states of each bridge cannot occur in the same sampling interval, the above equation becomes:

$$\delta_H = \frac{|V_x| + V_x}{2V_H}, \delta_H = \frac{|V_x| - V_x}{2V_L} \tag{7}$$

Formula（5）becomes：

$$\begin{cases} i_H = \varphi_H i_u + \psi_H i_v + \xi_H i_w \\ i_L = -\left(\varphi_L i_u + \psi_L i_v + \xi_L i_w \right) \end{cases} \tag{8}$$

From equations (4) and (8), the following relationship can be obtained:

$$\frac{dx}{dt} = Bu \tag{9}$$

Where $x = V_M$, $B = \frac{1}{C}\left[-i_u, i_u, -i_v, i_v, -i_\tau, i_\tau\right]$ $u = \left[\varphi_H, \varphi_L, \psi_H, \psi_L, \xi_H, \xi_L\right]^T$.

From the analysis, it can be seen that for a given reference voltage, the DC-link voltage can be balanced by properly adjusting the sum.

3. NPC INVERTER MIDPOINT POTENTIAL CONTROL

In this paper, the proportional control and a suitable PWM technology are combined to realize the smooth control of the midpoint potential of the diode clamp type three-level inverter, avoiding the unnecessary jitter in the midpoint potential adjustment process. In order to avoid the midpoint voltage fluctuation problem that arises in the control process of the traditional voltage control method, two additional currents i_S and i_P are introduced, where i_P represents the equivalent current source current, and i_S is determined by i_P and i_M. The definition of i_P is given below, i_M can be obtained from the operation of the midpoint voltage through the proportional controller, where the proportionality factor k is determined by the bandwidth and capacitance of the DC link. The control flow diagram of the control method is shown in Figure 2.
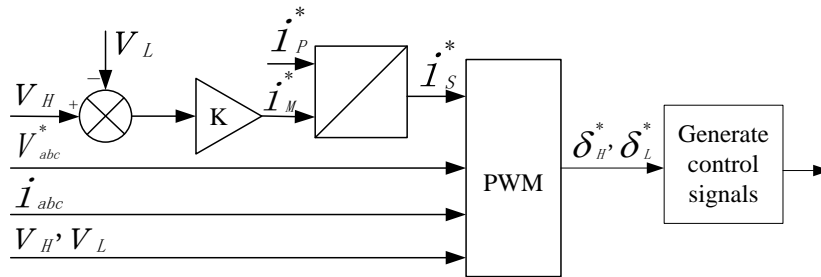
Figure 2. Control flow diagram based on proportion

Substituting equation (7) into equation (8):

$$\begin{cases} i_H = \dfrac{1}{2V_H}\left(\sum_x |V_x| i_x + \sum_x V_x i_x\right) \\ i_L = -\dfrac{1}{2V_L}\left(\sum_x |V_x| i_x - \sum_x V_x i_x\right) \end{cases} \tag{10}$$

Based on this, introduce two DC-link currents i_P and i_S, their definitions are as follows:

$$\begin{cases} i_P = V_H i_H + V_L i_L = \sum V_x i_x \\ i_s = V_H i_H - V_L i_L = \sum |V_x| i_x \end{cases} \tag{11}$$

Where i_P represents the equivalent current source current, which is proportional to the active power, but i_S is the auxiliary current determined by i_P and i_M, and the relationship is as follows:

$$i_s^* = (V_H - V_L)\cdot i_P^* + (2V_H V_L)\cdot i_M^* \tag{12}$$

Therefore, it does not affect the power exchange between the photovoltaic system and the main AC grid, and $\dot{i}_S$ can be set according to the need of the DC-link equivalent voltage. A suitable $\dot{i}_M^*$ is as follows:

$$\dot{i}_M^* = -K V_M \tag{13}$$

In order to achieve proper dynamic performance, it is necessary to set the K, $\dot{i}_M^*$ can be set as $\dot{i}_M$, especially when compared with the DC-link voltage its change is almost instantly completed. The bandwidth of the unbalanced voltage control loop of DC link is set as f_{DC}, K can be expressed as follows:

$$k = 2\pi f_{DC} C \tag{14}$$

K and $\dot{i}_S^*$ are deduced from the above analysis.

3.1. PWM control technology

In order to realize the control of the midpoint potential of the inverter, a suitable PWM technique is needed, and tracking of $\dot{i}_S$ can be achieved through this PWM technique. The flow chart of PWM control technology is shown in Figure 3.
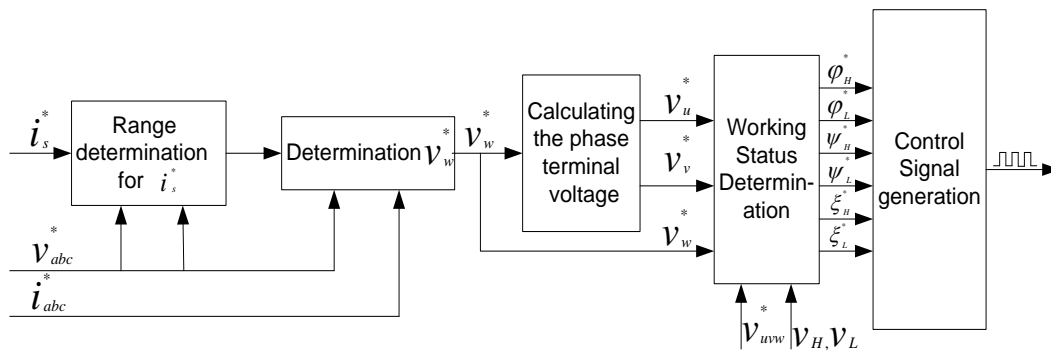
Figure 3. Ratio-based PWM control flow diagram

Considering the reference chain voltages of u, v, and w cells, which can be expressed as follows:

$$V_{uv}^* = V_u - V_v, V_{vw}^* = V_v - V_w, V_{wu}^* = V_w - V_u \tag{15}$$

It can be derived from the above formula:

$$V_u = -V_{wu}^* + V_w, V_v = V_{vw}^* + V_w \tag{16}$$

By substitution of (16) to (6):

$$V_{w,\min} \le V_w \le V_{w,\max} \tag{17}$$

Where:

$$\begin{cases} V_{w,\min} = \max\left\{V_{wu}^*, -V_{vw}^*\right\} - V_L \\ V_{w,\max} = \min\left\{V_{wu}^*, -V_{vw}^*\right\} + V_H \end{cases} \qquad (18)$$

It can be determined that the setting of the reference voltage can be realized for any V_M that meets the requirements, and by substitution of (17) to (11):

$$\begin{cases} i_P = -V_{wu}^* i_u + V_{vw}^* i_v + V_w\left(i_u + i_v + i_w\right) \\ i_S = \left|-V_{wu}^* + V_w\right| i_u + \left|V_{vw}^* + V_w\right| i_v + \left|V_w\right| i_w \end{cases} \qquad (19)$$

Therefore, assuming that the sum of the phase currents is equal to zero, it can be found that in the the three-phase system with isolated star connection, the change of i_P does not depend on V_M. Therefore, i_S can control V_M according to the demand of the DC-link voltage without affecting the energy exchange between the photovoltaic system and the main AC grid.

For the control of i_S to be implemented, voltage and current sectors need to be considered. In the parity sector, (18) can be changed to:

$$\begin{cases} V_{w,\min} = -V_{vw}^* - V_L, V_{w,\max} = V_{wu}^* + V_H \\ V_{w,\min} = V_{wu} - V_L, V_{w,\max} = -V_{vw}^* + V_H \end{cases} \qquad (20)$$

Based on the value of each (δ_v, δ_i) in (20), the alternative relation of i_S and V_M can be determined. It can be seen that the minimum and maximum values of i_S that can be seen from here are usually in correspondence with V_w^+ or V_w^-, and they are defined as:

$$\begin{cases} V_w^{(+)} = \max\left\{V_{wu}^*, -V_{vw}^*\right\} \\ V_w^{(-)} = \min\left\{V_{wu}^*, -V_{vw}^*\right\} \end{cases} \qquad (21)$$

Therefore, if there is at least one of V_M is in the interval $\left[V_{w,\min}, V_{w,\max}\right]$, it means that the plateau region of i_S will appear. As previously assumed, since the sum of the currents of the phases in this region is equal to zero, the change of V_M does not affect the value of i_S. When V_W is equal to zero, the maximum or minimum of i_S in current sector II and V occurs. In this case, a given i_s^* may correspond to two different values: V_w^* and $\tilde{V}_w^*$. To ensure linear control of i_S over its full range and that V_w^* is within the V_w^* time period. V_w^* should be selected. In conclusion, for the given V_M and i_s^*, we can choose V_w^* according to the analysis above, all the phase terminal voltages are calculated by formula (16), and the duty cycle of each bridge in the H and L states can be calculated by (7).

4. SIMULATION ANALYSIS

In order to verify the feasibility of the proposed method, a system simulation model was set up in MATLAB. Set the DC-link voltage to 1.5KV, the switching frequency to 10KHz, the sampling interval to 100us, the minimum pulse width to 0.8us, the power supporting the photovoltaic system is 30KVA, and the high and low side capacitor voltages of DC-link are set to 0.6pu and 0.4 respectively. The simulation results are as follows. Figure 4 and Figure 5 show the changes of the midpoint voltage and current respectively. Figure 6 and Figure 7 show the voltage and current waveforms of the inverter input to the power grid respectively. The simulation results show that the method achieves the smooth control of the midpoint potential. At lower voltage and current ripples,

the stability of the midpoint potential control is ensured when the power changes, ensuring the quality of the electrical energy input to the grid. Harmonic detection output by inverter is controlled within 0.04.
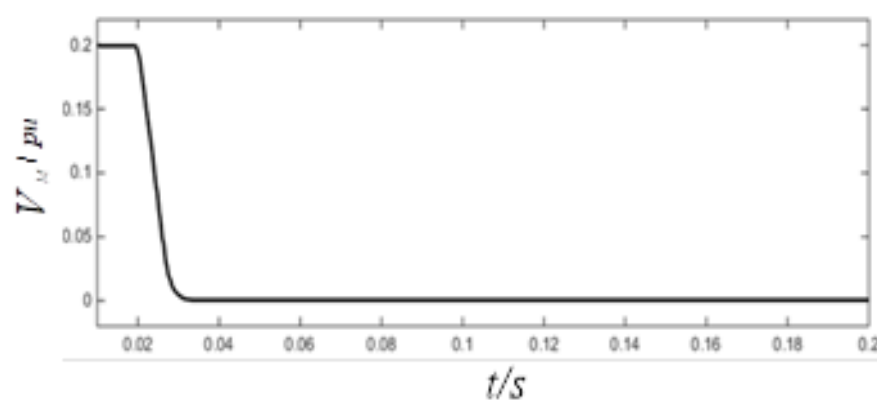
Figure 4. Midpoint potential change curve
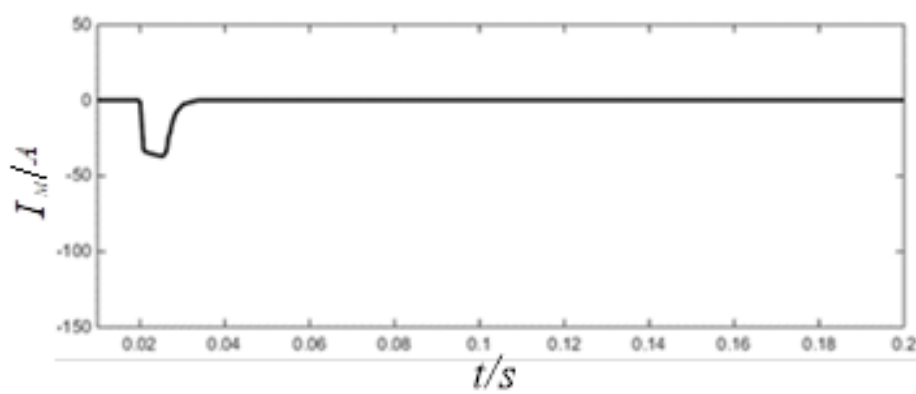
Figure 5. Midpoint current curve
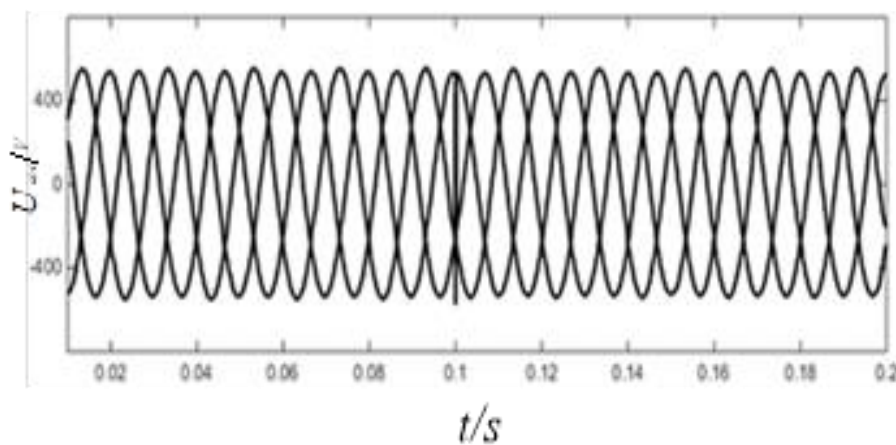
Figure 6. AC line voltage curve
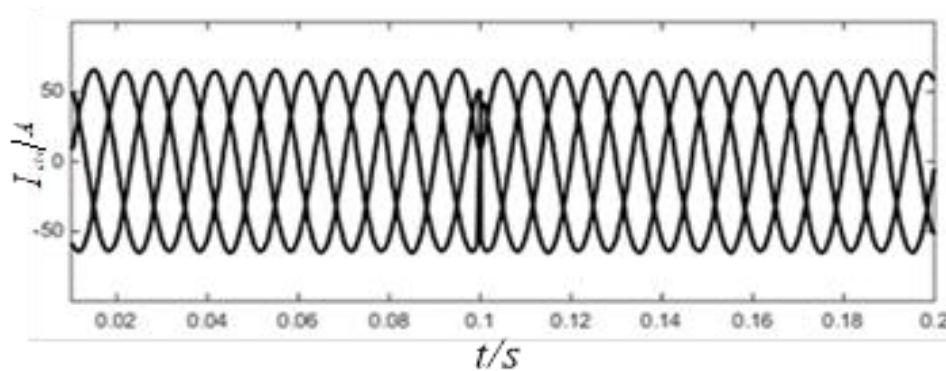
Figure 7. AC phase current curve

5. CONCLUDING REMARKS

The scheme based on the proportional controller proposed in this paper, through the design of the proportional controller, combined with a new PWM technology to control the midpoint potential. The simulation results show that the method effectively suppresses the drift of the DC side capacitor voltage, reduces the ripple of voltage and current in the output power, and realizes the effectiveness of the midpoint potential control, and the harmonics input by the inverter to the grid energy are also within acceptable limits.

REFERENCES

[1] Irwanto, M., et al. "Effect of Maximum Voltage Angle on Three-Level Single Phase Transformerless Photovoltaic Inverter Performance." *Telkomnika Indonesian Journal of Electrical Engineering* 12.8(2014).
[2] Chun-Yu, X. U., and M. Liu. "Study of Neutral-point Potential Control Method for Three-level Inverter."*Electric Drive*(2013).
[3] Xing, L. I., et al. "A New Neutral Voltage Balance Control Strategy of Three-level NPC Inverter." *Journal of Power Supply* (2016).
[4] Ibrahim, Zulkifilie Bin, et al. "Comparative Analysis of PWM Techniques for Three Level Diode Clamped Voltage Source Inverter." *International Journal of Power Electronics & Drive Systems* 5.1(2014).
[5] Vaseee, Srinu, and B. V. Sankerram. "Voltage Balancing Control Strategy in Converter System for Three-Level Inverters." *International Journal of Electrical & Computer Engineering* 3.1(2013):7-14.
[6] Cai, Jiang, et al. "A Neutral-point Voltage Balancing Control Method for Three-level Neutral-point-clamped Inverter." *Automation of Electric Power Systems*38.7(2014):88-94.
[7] Hashir, Shaziya, Jebin Francis, and R. Sreepriya. "A novel hybrid PWM method for DC-link voltage balancing in a three level neutral point clamped inverter." In *2018 International Conference on Power, Signals, Control and Computation (EPSCICON)*, pp. 1-6. IEEE, 2018.
[8] Gang, Liu, Wang Dafang, Wang Miaoran, Zhu Cheng, and Wang Mingyu. "Neutral-Point Voltage Balancing in Three-Level Inverters Using an Optimized Virtual Space Vector PWM With Reduced Commutations." *IEEE Transactions on Industrial Electronics* 65, no. 9 (2018): 6959-6969.
[9] Kashif, Muhammad, et al. "A Study of Three-Level Neutral Point Clamped Inverter Topology." *Telkomnika Indonesian Journal of Electrical Engineering* 12.8(2014).
[10] Zhong, Wan Sheng, et al. "Control Strategy of Neutral-point Potential Balancing in Three-level Inverter." *Electric Drive* (2014).
[11] Cao, Guofeng, R. Wang, and R. Meng. "Integrated control strategy of neutral point potential balance in three-level inverter." *Modern Electronics Technique* (2017).
[12] LI Xing, JIN Bin, XIONG Ming, WANG Jianlin. A New Neutral Voltage Balance Control Strategy of Three-level NPC Inverter[J], *Journal of Power Supply, 2017,40(16):165-169*
[13] J. S. Lee and K. B. Lee, "New Modulation Techniques for a Leakage Current Reduction and a Neutral-Point Voltage Balance in Transformerless Photovoltaic Systems Using a Three-Level Inverter," in *IEEE Transactions on Power Electronics, vol. 29, no. 4, pp. 1720-1732, April 2014.*
[14] Gnanasundari, M., M. Rajaram, and Sujatha Balaraman. "Natural balancing of the neutral point potential of a three-level inverter with improved firefly algorithm." *Journal of Power Electronics.16, no. 4 (2016): 1306-1315.*

[15] W Keli, X Changliang, Z Yun. Common-mode voltage suppression for neutral-point-clamped three-level inverter. *Transactions of China Electrotechnical Society,30(24), pp.110-117.*

[16] Jianguo, L., Wenbin, H. and Fuyun, W. Low frequency oscillation suppression scheme of neutral-point voltage for neutral point clamped three-level inverter. *Proceedings of the CSEE, 35(19), pp.5039-5049.*

[17] Karthikeyan, D., R. Palanisamy, K. Vijayakumar, A. Velu, and D. Selvabharathi. "Parallel Connected VSI Inverter using Multi-carrier based Sinusoidal PWM Technique."*Telkomnika 15, no. 4 (2017): 1625-1631.*

[18] Tong, Jun, Jianwei Qiao, Lijun Liu, Yao Lu, and Qian Zhang. "Neutral point potential balance control strategy of three level inverter." *In 2018 13th IEEE Conference on Industrial Electronics and Applications (ICIEA), pp. 1357-1361. IEEE, 2018.*